THE USE OF SEMICONDUCTOR DEVICES IN NUCLEAR SPECTROSCOPY

by

DUANE K. FOWLER

B. A., University of South Dakota, 1961

A MASTER'S THESIS

submitted in partial fulfillment of the

requirements for the degree

MASTER OF SCIENCE

Department of Physics

KANSAS STATE UNIVERSITY
Manhattan, Kansas

1963

Approved by:

Louis D. Ellsworth

Major Professor

LD
2668
T4
1963
F69
C.2
Document

TABLE OF CONTENTS

INTRODUCTION....1

THEORY....2

APPARATUS....16

DISCUSSION AND EXPERIMENTAL RESULTS....18

CONCLUSION....63

ACKNOWLEDGEMENTS....64

LITERATURE CITED....65

INTRODUCTION

In recent years, semiconductor devices have been developed which have already had widespread application in the detection of charged particles. The production of these devices was an outgrowth of earlier work on the crystal counter, which did not prove successful as an energy spectrometer because of polarization and the non-uniformity of pulse height distribution for mono-energetic particles.(12) Semiconductor detectors have exhibited good energy resolution and linearity over a wide energy range. While they cannot match the resolution of magnetic spectrometers, their small size, relatively low cost, simple power requirements, and adaptability to specific applications make them much more practical than the cumbersome spectrometer. Semiconductor detectors are especially adapted for the detection of fission fragments, alpha particles, deuterons, protons, and electrons. They have a relatively low direct sensitivity to photons and neutrons. The reader is referred to D. A. Bromley's article (3) for a good account of the many, diversified applications of semiconductor detectors in nuclear experimentation as of 1962.

Three main types of detectors have been fabricated thus far: 1) the diffused p-n junction diode; 2) the surface barrier diode; and 3) the p-i-n semiconductor detector. A fourth type, the bulk conductivity counter, is under study.(13) The Nuclear Physics group at Kansas State University has obtained and used each of the three main types of detectors primarily for the detection of internal conversion electrons in the study of nuclear decay schemes.

THEORY

Essential to the understanding of the operation of a semiconductor detector, or, for that matter, any semiconductor device, is the concept of impurity concentrations in semiconductors, and the theory of a p-n junction. Therefore, these topics will be discussed first. It will be assumed the reader is familiar with the electron energy band theory.

Germanium (Ge) and silicon (Si) are typical semiconducting materials, in that the forbidden energy gap between the valence band and the conduction band is small: 0.72 ev for Ge and 1.11 ev for Si. Both elements are tetravalent and crystallise in the diamond structure.(20) This means each Ge or Si nucleus, along with its filled inner shells of electrons, is surrounded by four electrons. These four electrons are shared by the atom's four nearest neighbors, but the atom receives, in return, a share in one valence electron from each neighbor. Each atom, therefore, has eight valence electrons associated with it. These electrons completely fill the valence band. At absolute zero, all of the electrons remain in the valence band, but as the band is completely filled, the electrons cannot contribute to current conduction. As the temperature increases, a few of the electrons will obtain enough energy from thermal collisions to jump into the empty conduction band. Now, the electrons in the conduction band and the holes in the valence band can contribute to current conduction because the bands are neither completely filled nor completely empty. This is called intrinsic conduction.

If an atom of a pentavalent substance, such as phosphorus (P), replaces a Si or Ge atom in the crystal, four of the valence electrons will enter into the sharing arrangement with the nearest neighbors as described above. However, there is no position available for the fifth valence electron in the valence band. The consequence is the creation of an energy level in the forbidden energy gap very close to the lower edge of the conduction band. This indicates that this electron is very loosely bound to a P atom, and only a small amount of thermal energy is required to kick it up into the conduction band. At absolute zero, the conduction band is still empty, but at a very low temperature nearly all of the impurity atoms have been ionized; i.e., the extra valence electrons have been thermally activated to the conduction band, greatly increasing the conductivity of the crystal impurity. If a semiconducting material has such a pentavalent impurity present, it is called n-type material, and the impurity is called a donor impurity because it donates electrons to the empty band.

If a trivalent atom, such as boron (B), replaces a Si or Ge atom, one of the valence bonds is incomplete. A new energy level is created, again in the original forbidden gap, but this time it is very close to the top of the valence band. Consequently, very little thermal energy is needed for a B atom to acquire an electron from one of its Si or Ge neighbors. There is now an electron deficit in the valence band, which may migrate from atom to atom as a positive hole, or vacancy. Conduction by holes is then possible in the valence band. An impurity of

this type is called an acceptor impurity, since it accepts electrons from the valence band. A semiconductor containing an acceptor impurity is called p-type material.

Figure 1 illustrates an energy level diagram of a semiconductor having both donor and acceptor impurities.

Figure 1

It is interesting to examine the effect of impurities on the conductivity, σ, of a crystal, which is a measure of the ability to support a current flow. The complete equation for conductivity is:

$$\sigma = n \mu_n q + p \mu_p q \tag{1}$$

where n and p are the number of electrons and holes per cc in the conduction and valence band, respectively; μ_n and μ_p are the mobilities of the electrons and holes, respectively; and q is the charge of an electron or hole.(17) For an intrinsic semiconductor,

$$n = p \simeq e^{-E_g/2KT} \tag{2}$$

For a semiconductor containing a donor impurity,

$$n \simeq \sqrt{N_d}\; e^{-(E_g - E_d)/2KT} \tag{3}$$

where N_d indicates the concentration of donor atoms per cc. For a p-type material,

$$p \simeq \sqrt{N_a}\; e^{-E_a/2KT} \tag{4}$$

As can be seen from Figure 1, E_a and $E_g - E_d$ are very much less than E_g. Therefore, the conductivity is greatly increased by the addition of only a small concentration of impurity. The resistivity, ρ, which is the reciprocal of conductivity, is accordingly reduced.

By way of definition, a p-n junction is the region that exists between n-type material and p-type material when the two types are present in a single crystal. Although one must grow a p-n junction, it is illustrative in the study of p-n junctions to consider the situation when isolated samples of n-type and p-type material are brought into contact. Since electrons are more populous in the conduction band of the n-type material than in the p-type material, a concentration gradient exists and electrons will diffuse from the n-type region to the p-type region. A similar hole concentration gradient exists in the valence band and holes will migrate from the p-type region to the n-type region. The p-type region, then, becomes negatively charged and the n-type region positively charged and a potential difference is established across the junction. The potential difference is in such direction to oppose the further diffusion of holes and electrons. Equilibrium is established when the potential difference is just large enough to balance the tendency of more electrons and holes to diffuse across the junction. The potential difference, typically, has values of 0.01 v to 1 v, depending on the impurity content of the material. The contact potential results in the relative downward displacement of the energy levels of the n-type region.

However, the edges of the energy bands do not form an abrupt discontinuity at the junction, but rather go through a tapered step. This is illustrated in Figure 2. The slope of this step is the magnitude of the electric field in the junction due to the potential difference. The region within which the field exists, commonly referred to as the p-n junction barrier, is generally 10^{-4} to 10^{-6} cm wide.(18)

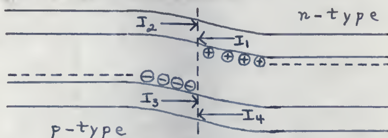

Figure 2

It would be profitable to examine in more detail the distribution of charges that gave rise to the potential difference. The electrons, which flowed from the n-type material to the p-type material when the two specimens were brought into contact, are to be found occupying all the available acceptor levels a short distance from the junction. The holes which flowed from the p-type region to the n-type region recombine with electrons on the n-type side and result in the complete emptying of the donor levels for a short distance on the other side of the junction. This complete ionization of the acceptor and donor levels next to the junction gives a double layer of charge which establishes the potential difference.(18) In Figure 2, the encircled minus signs indicate filled acceptor levels, and the encircled plus signs indicate empty donor levels. The charge density of this space charge region is illustrated in Figure 3.

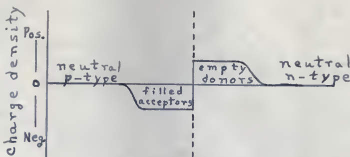

Figure 3

Under equilibrium conditions, no net current flows across the junction, although currents of both holes and electrons continue to flow in both directions across the junction. These currents can be considered as four separate components, which are labelled I_1, I_2, I_3, and I_4 in Figure 2. (Conventional current directions apply.) In the diffusion process, electrons moving from n-type to p-type material and holes moving from p-type to n-type material are designated as majority carriers. Electrons and holes moving in the opposite direction are termed minority carriers. Although minority carriers must diffuse to the edge of the junction, they represent drift currents because the electric field pulls them across the junction. Thus, I_2 and I_3 represent current flow by majority carriers, and I_1 and I_4 represent current flow by minority carriers.(18)

If, now, a voltage is applied to the diode such that the n-type region is made positive and the p-type negative with respect to each other, the diode is said to be reverse biased. A voltage applied in this way simply adds to the potential difference that exists across a junction in equilibrium. The applied field tends to pull both types of carriers away from the barrier (holes on the p-type side and electrons on the n-type

side), thus extending the space charge layer. This layer has a low concentration of carriers; therefore, its resistivity is high, and practically all the applied voltage appears across the barrier.(4) The barrier voltage step is heightened accordingly, as shown in Figure 4.

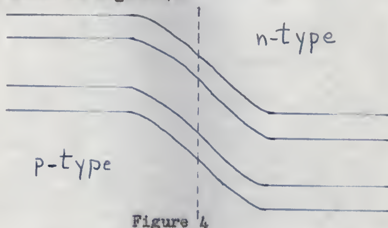

Figure 4

The space charge region is, in effect, a parallel plate capacitor with a dielectric between the plates. The distance between the plates is the width of the barrier.

It is apparent from Figure 4 that the increased height of the barrier will greatly reduce the current components I_2 and I_3. However, I_1 and I_4 depend upon the diffusion of minority carriers to the junction, and hence are independent of the applied voltage. If the reverse bias is sufficiently great to make I_2 and I_3 negligible, the sum of I_1 and I_4 constitutes the reverse saturation current of the junction which is theoretically independent of the applied voltage.(18)

The diffused p-n junction diode that is used as a charged particle detector is very similar to the diode just discussed. The most common practice is to form a p-n junction close to one surface of a high resistivity p-type silicon slab by a shallow diffusion of phosphorus. Detectors have also been made by

diffusing boron into n-type silicon.(10) Details of construction techniques, making electrical contacts, and mounting of the diode will not be discussed here.

When a reverse bias is applied to the diode, a space-charge region is established on both sides of the junction. The width, X, of this depletion layer is given by $X = X_p + X_n$ where X_p and X_n are the extent of the depletion layer into the p-type and n-type material, respectively, from the junction. Either X_p or X_n are given approximately by

$$X = \left(\frac{\epsilon V}{2\pi q N_I}\right)^{1/2} \qquad (5)$$

where V is the total potential drop across the depletion layer, ϵ is the dielectric constant of Si, q is the electronic charge, and N_I is the concentration of ionized impurity centers in the appropriate type material. X_p/X_n typically has a value of 10^3, as $X_p/X_n = (\sigma_n/\sigma_p)^{\frac{1}{2}}$.(7) A good approximation of Equation 5 is $X = \frac{1}{3}(\rho V)^{\frac{1}{2}}$, where X is in microns if ρ, the resistivity of the p-type material, is in ohm cm and V is in volts.(15) The capacitance is given by

$$C = \frac{\epsilon A}{X} = 1.06 \times 10^4 \frac{A}{X}\ pf \qquad (6)(1)$$

showing that C is inversely proportional to $(V)^{\frac{1}{2}}$. A is the area of the device in cm^2; X is the depth of the depletion layer in microns.

A charged particle, incident upon a semiconductor, produces hole-electron pairs by inelastic collisions in much the same way as electron-ion pairs are produced in a gaseous ionization chamber. It is found that, on the average, 3.5 ev of incident particle energy is needed to produce one hole-electron pair in Si, as compared to 2.94 ev in Ge. Fortunately, all experimental

evidence indicates that these figures are independent of the mass of the incident particle, hence the type of particle. To be useful as an energy spectrometer, then, the device must be able to give some indication of the number of electron-holes that are produced by the incident particle. The reverse-biased p-n junction diode meets this requirement, subject to the restriction discussed in the next paragraph. An electric field produced in the depletion layer by the applied voltage causes electron-hole pairs created in this region to be swept out of the depletion layer and to be collected on the "plates" of the parallel-plate capacitor, appearing as a voltage pulse. The height of the pulse is determined by $V = Q/C$ where Q is the total charge collected and C is the sum of the capacitance of the detector and the input capacitance of the amplifier being used. If a charge sensitive amplifier is used, C is just the input capacitance; i.e., V is independent of the detector capacitance. The rise time of the pulse is of the order of nanoseconds; the decay time is determined by the RC time constant of the circuit.(8)

Any electrons or holes created outside the depletion layer must diffuse to that region before they can contribute to the signal, as the electric field exists only in the depletion layer. Miller reports that the time for a carrier to diffuse L microns is $T = L^2$ nanoseconds, with the result that it takes approximately 100 times longer to collect charge by diffusion than by drift.(15) If the diffusion times are longer than the RC time constant of the system, the pulse height will not represent the energy lost by the particle. Therefore, to be a successful energy detector,

the depletion layer of the diode must be greater than the range of the particle to be detected. In addition, there must be a negligible dead layer or window through which the particle passes before reaching the depletion layer. A thick depletion layer is also necessary to minimize the capacitance of the detector, thereby increasing the voltage pulse height output and giving a better signal-to-noise ratio.

In view of the results of the preceding paragraph and the fact that $X \alpha (\rho V)^{\frac{1}{2}}$, it is evident that the important condition that must be met in a p-n junction diode is the optimizing of the ρV product. The maximum voltage that may be applied is determined by the noise level of the device, which is dependent on the reverse current as shown in Equation 7.

$$V^2 = \frac{2 q I \Delta f}{\omega^2 C^2} \qquad (7)$$

V^2 is the mean square noise voltage; I is the reverse current; Δf is the frequency bandwidth; and $1/\omega C$ is the impedance.(22) Miller has shown that the reverse current varies approximately as the depth of the depletion layer, or as the square root of the applied bias. This implies that the reverse, or leakage current, is largely due to the thermal generation of carriers in the space charge region.(15) Another source of reverse current is the flow of minority carriers across the junction discussed earlier. The total reverse current for lightly doped n-type silicon is given by

$$I \simeq 6.4 \times 10^{-14} \frac{\rho^{1/2} V^{1/2}}{\tau} + 4.7 \times 10^{-14} \frac{\rho}{\tau^{1/2}} \ \frac{\text{amperes}}{\text{cm}^2} \qquad (8)(14)$$

where τ is the minority carrier lifetime; i.e., the average time a minority carrier exists before recombining with a majority carrier. The reverse current in lightly doped p-type

silicon is

$$I \simeq 3.8 \times 10^{-14} \frac{\rho^{1/2} V^{1/2}}{\tau} + 1.7 \times 10^{-14} \frac{\rho}{\tau^{1/2}} \frac{\text{amperes}}{\text{cm}^2} \quad (9)(14)$$

It is apparent that τ must be kept as long as possible. One disadvantage of the p-n junction diode is that the high temperature required for the diffusion process tends to decrease the minority carrier lifetime. As the total barrier leakage current is proportional to the diode area, p-n junction diodes usually have small areas.

The resistivity is the other variable which must be large in order to obtain a wide depletion layer. The limit of this factor is usually the availability of high resistivity silicon, as silicon with resistivity greater than 10,000 ohm cm is difficult to produce. Also, from Equation 8 and 9, it is seen that the leakage current increases with resistivity, thereby prohibiting the use of very high resistivity silicon, if it were available.

Considering the limits on the applied bias and the resistivity of the p-type silicon, typical depths of depletion layers so far obtained are 200-500 microns. Miller obtained a depletion layer 700 microns deep, using 13,000 ohm cm silicon and using a bias of 400 V. Essentially windowless detectors have been fabricated by diffusing to a depth of only 0.1 micron.(15)

Nearly all of the discussion on the diffused p-n junction diode applies to the surface barrier diode, except the method of producing the junction. In this case an inversion layer is formed just below the surface of a semiconductor that has a different conductivity type than the bulk material. An inversion layer does not result from doping the material with an

impurity; it results, rather, from a net surface charge. For example, if a slab of n-type material acquires a net negative surface charge, the electrons in the conduction band will be repelled from the surface and holes in the valence band will be attracted to it, producing a thin, p-type inversion layer just below the surface. This layer is generally 10^{-4} to 10^{-6} cm thick. To produce electron traps, the surface of the crystal is simply exposed to oxygen and steam or ozone and steam.(1) Boron trifluoride and chlorine can also be used to produce a negative surface charge.(9)

The most common surface barrier diode detector is fabricated from n-type silicon. This detector has several advantages over the diffused p-n junction diode, including a negligible dead layer, simpler construction techniques, and the elimination of deleterious heating. Accordingly, the leakage current is small and larger area devices can be made. In general, the surface barrier diode has a narrower depletion layer than the diffused p-n junction detector. A better approximation for the width of the depletion layer in a surface barrier detector is $X = \frac{1}{2}(\rho V)^{\frac{1}{2}}$.(13)

The biggest limitation in the use of diffused p-n junction and surface barrier detectors is the thin depletion layers that are attainable. The p-i-n junction detector has eliminated this restriction, by providing a sensitive region up to 6 mm thick.(13)

This wide depletion layer is achieved by using the lithium drift process.(16) First, a p-n junction is formed by diffusing lithium, which is an interstitial donor impurity, into low

resistivity p-type material. Only 0.03 ev is needed to ionize the lithium atom in a silicon crystal, so essentially all the Li atoms are ionized. If a reverse bias is applied to the diode at an elevated temperature, the Li^+ ions are found to have sufficient mobility to drift in the electric field. Thus, the Li^+ ions close to the junction move to the other side of the junction. The electrons, although not actually being bound to the atom, are still in some way associated with the atoms so they move with the ions. The Li donors compensate the acceptors of the original p-type material, usually B, and produce an intrinsic region between the n-type and p-type regions. The intrinsic region is the sensitive region of the device and is analagous to the depletion layer in a junction detector. An advantage of this type detector is that low resistivity p-type Si, 0.1 to 3000 ohm cm, can be used.

One of the drawbacks of the first units constructed was the presence of a thick, n-type dead layer through which the particles had to traverse to reach the sensitive region. This problem has been overcome by drifting the Li almost completely through the p-type region to the electrical contact on the back surface and then using this surface as the entrance for charged particles.(2)

Though the p-i-n detector is operated with a reverse bias to establish the electric field that collects the hole-electron pairs, the depth of the sensitive region is practically independent of the voltage. C varies as $V^{-1/3}$ for low voltages and then approaches a constant value, as compared to the $V^{-\frac{1}{2}}$ dependence in a junction detector.(24)(13) The rise time of the voltage

pulse output is dependent on the bias, indicating that a larger bias decreases the time of collection.

In addition to the references already indicated, Harry Mann at Argonne National Laboratory has had considerable experience in the construction and testing of the lithium ion drift detectors.(11)

As indicated previously, a problem in semiconductor detector technology is to keep the noise level as low as possible. In addition to the reverse current as a source of noise, there is noise contribution due to surface leakage currents across the edge of the junction. Some attempts have been made to protect the junction edge with oxide layers(15), a polystyrene solution dissolved in toluene(1), or with a guard ring construction.(6) Another method for reducing the detector noise to a negligible value has been to cool the detectors to liquid nitrogen temperature, 77° K. No damage to a detector has been reported as a result of cooling, although some trouble has been encountered with particular types of mounting. Epoxy potted detectors have proven to be unsuitable because the large difference of expansion coefficients caused separation of the Si and epoxy upon cooling.(21)

APPARATUS

The complete system used in conjunction with semiconductor detectors as energy spectrometers is illustrated by the block diagram in Figure 5.

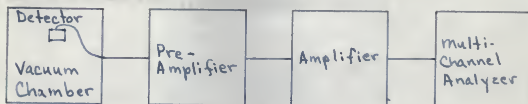

Figure 5

The vacuum chamber was simply a rectangular box constructed of 3/16 inch brass plates soldered together. One face was used as a door which, during operation, was held in place by atmospheric pressure on the outside, a seal being made by a neoprene O-ring coated with Apiezon vacuum grease. Electrical connections were made through glass seals. The detectors were mounted on a copper rod soldered in the back side of the vacuum chamber and extending through the side into a liquid nitrogen container, which was a tin can with rolled seams. The detectors were cooled by keeping the copper rod immersed in liquid nitrogen. For thermal insulation, the vacuum chamber and liquid nitrogen reservoir were enclosed with 2 inches of styrofoam, having a thermal conductivity of 0.37 milliwatts/cm °K at room temperature.(23)

The preamplifier and the amplifier were designed by Instruments Development Products (IDP) specifically for use with solid state detectors. The preamplifier is a charge sensitive amplifier with a gain of 400. The original input stage used a nuvistor, type 7586, but this was replaced by a special purpose tube, 7788, lowering the noise level and producing an increase in the

resolution of the system from 12 Kev to 8 Kev. The resolution of the system was determined by shorting the detector input, feeding the system the output of a pulser contained in the IDP unit, and measuring the full width at half maximum of the peak obtained on the multichannel analyzer. The noise level was measured on an oscilloscope at the output of the preamplifier. All noise levels stated hereafter in this paper were measured at this point. With the input shorted, the noise level had a value of 15-20 mv.

The amplifier actually consists of two isolated units, labelled the main amplifier and the post amplifier. The gain of each is separately adjustable. The post bias between the two units can be used to reject noise or small pulses such that only those pulses above the bias setting are received and amplified by the post amplifier. The post bias effects a spreading out of the spectrum. An output can be taken from either the main amplifier or the post amplifier, but in most instances it is advantageous to use the post bias and post amplifier output. The output of either unit is 0-100 v, positive.

The multichannel analyzer used was a Nuclear Data, ND 130A, 512 channel analyzer. The 0-100 v positive or bipolar input was used.

DISCUSSION AND EXPERIMENTAL RESULTS

One p-n junction diode used at Kansas State University was purchased from Solid State Radiations, Inc. The junction was formed by a shallow diffusion of phosphorus into p-type silicon of 1.73 X 10^4 ohm cm resistivity. This detector has a sensitive area of 0.4 cm^2 and is surrounded by a guard ring structure to protect the junction edge and reduce the effects of surface current leakage across the junction. The guard ring was formed by etching a groove completely through the n-type layer and the junction, thereby isolating the guard ring from the effective detector region. Pulses and noise generated in the guard ring are by-passed through the battery circuit and do not go to the preamplifier. The manufacturer estimates the depth of the sensitive region to be 310 microns at the maximum operating voltage of 50 v, determined from a capacitance measurement, and the window, or dead layer, to be one micron. Using the approximate equation, $X = \frac{1}{3}(\rho V)^{\frac{1}{2}}$, the same value of 310 microns is obtained for the depth of the sensitive region at 50 v.

This detector exhibited a low noise level and good resolution. Typical noise levels for this detector were: no bias, exposed to light, 200 mv; no bias, in a light-tight box, 150 mv; 20-50 v bias, 30 mv. After several hours of operation, the noise level would increase slightly, but never would it go over 40 mv. The resolution was consistently 15 Kev full width at half maximum, and was independent of energy. The effective electron energy range for this detector was 30-400 Kev, indicating that

the depth of the sensitive region may be greater than 310 microns.

This detector was cooled to 77° K only once, and then for a short time only. The noise level was reduced to 20 mv, which indicated that the detector was contributing very little, if any, to the noise level. It was estimated that the resolution improved to 9 or 10 Kev. The resin that was used to hold the detector in its aluminum frame became very discolored, cracked, and flaked off in a few places. For this reason, it was not deemed advisable to cool it again. The detector, itself, apparently was not damaged as it continued to give the same noise level and resolution as it had prior to cooling.

A diffused p-n junction diode detector, purchased from RCA Victor Company, Ltd., had a diffusion depth of only 0.2 micron and an insensitive region of approximately 0.1 micron, making the detector essentially windowless. The manufacturer quoted the resistivity of the p-type material to be of the order of 10^4 ohm cm, but furnished no figures on the depth of the sensitive region. The detector was found to be sufficiently thick to stop 350 Kev electrons at 70 v bias, the maximum operating voltage. It was necessary to operate the detector at 70 v bias for electron energies greater than 200 Kev in order to make the depletion layer deep enough to collect their full energy.

The noise level was comparable to the other detectors; at 0 bias, the noise level was 80 mv; at 40 v, 40 mv; and at 70 v, 50 mv. The resolution obtained at room temperature was 17 Kev, which was independent of energy.

This detector was cooled several times, and did not appear to have suffered any harmful effects. Since the only direct thermal contact the detector had with the liquid nitrogen reservoir was through one lead wire, much of the cooling was accomplished by a radiative process, which is slower than heat conduction. It was found that at least one-half hour, and preferably one hour, should elapse from the start of the cooling process to the application of a bias. At 77° K, the noise level was 20 mv and 8-10 Kev resolution was obtained consistently. At room temperature, the low energy limit was 40 Kev; at 77° K, the limit was 15 Kev, which was determined by the noise level of the amplifier system.

The surface barrier diode, fabricated by Molechem, Inc., was not used to any great extent, and a full discussion of its characteristics and properties can not be given at this time. In the initial tests the detector performed much the same as the p-n junction diodes and produced a resolution of 18-20 Kev. Due to its mechanical construction, it was not thought advisable to cool this detector.

The lithium drifted p-i-n detector used at Kansas State University was furnished through the courtesy of Harry Mann at Argonne National Laboratory. The lithium was drifted almost completely through the 2 mm crystal, so the p-type side was used as the entrance. The window, composed of a thin dead layer of silicon and a gold film which provided the electrical contact, was determined to have an effective thickness of 25 microns. The crystal was 8 mm in diameter, but the mechanical holder restricted the effective area to 0.3 cm^2. With no bias,

the noise level was 100 mv; at 40 v, it was 40 mv; at 100 v, 50 mv; and at 200 v, the maximum recommended bias, the noise level was 60 mv. Although the noise level was lowest at 40 v, it was found to operate better at a higher bias, near 100 v. At 100 v, the output pulses had a shorter rise time and a more desirable shape for the multichannel analyser. No advantage was found for operating at a bias greater than 100 v, since the depth of the sensitive region is not a function of the applied bias in a p-i-n detector. Pulse shapes were not changed, and the resolution got worse as a result of the increased noise level at higher voltages. Due to the 25 micron window and the 50 mv noise level, 100 Kev was the minimum electron energy that could be detected. As the intrinsic region was nearly 2 mm thick, 1 Mev electrons could be detected easily. The resolution obtained with this detector was 30 Kev.

It was found necessary to cool the detectors with no bias applied. The first time a detector was cooled, a bias was applied to the detector prior to the start of the cooling process, resulting in an increase in the noise level with very violent and erratic bursts of noise being displayed on the oscilloscope at the output. Also, the resolution became worse than that obtained at room temperature. Thereafter, the detectors were cooled prior to the application of a bias, and the noise level decreased slowly and smoothly as the temperature decreased.

It is not known exactly why this phenomenon occured. One explanation might be that undue stresses are produced in the crystal when both temperature and electrical gradients exist

simultaneously, similar to the stresses obtained when pressure and electrical gradients exist simultaneously.

Because a charge sensitive preamplifier was used, the height of the output pulses was independent of the capacitance of the detector, and, therefore independent of the detector. The output pulses in mv were approximately equal to the electron energy in Kev. For example, a 50 Kev electron produced a voltage pulse height of 50 mv, and a 300 Kev electron produced a pulse height of 300 mv.

The energies lost by electrons traversing the windows of the various detectors, a function of the electron energy, are summarized in Table I. The figures were obtained by computing the slope of the electron energy versus range-in-silicon curve and using the values of the window thickness given by the manufacturer or determined experimentally.

Electron Energy in Kev	Energy lost in window in Kev		
	Argonne Detector	Solid State Rad. Detector	RCA Detector
1000	12	0.5	0.0
500	12	0.5	0.0
250	19	0.75	0.0
125	25	1.0	0.1
75	40	1.5	0.1
50	50	2.0	0.2
15	--	3.0	0.3
10	--	4.0	0.4

Table I

To construct a nuclear decay scheme for an isotope, it is necessary to determine the energies of transitions that take the excited nucleus to its ground state. There are two competing processes that are involved in this de-excitation of the nucleus; either a gamma ray may be emitted, or the nucleus

may directly transfer its energy to an orbital electron and eject it from its shell. This latter process is called internal conversion. The kinetic energy of the ejected conversion electrons is the energy of the transition minus the binding energy of the electron in its shell. The internal conversion coefficient, α, for a given transition is defined as the ratio of the number of conversion electrons to the number of gamma rays emitted in unit time; $\alpha = N_e/N_\gamma$. α is dependent on the energy of the transition, the atomic number of the isotope, and the type and multipolarity of the transition. Another useful quantity is the K/L ratio; i.e., the ratio of the number of conversion electrons ejected from the K-shell to the number ejected from the L-shell. Whenever a vacancy exists in the K-shell, either as a result of internal conversion or electron capture, it is usually filled by an electron from the L-shell, accompanied by the emission of an X-ray. However, instead of an X-ray being emitted, another electron may be ejected from the L-shell, leaving it doubly ionized. Electrons ejected from the atom in this way, called Auger electrons, have a kinetic energy of $E_K - 2E_L$, where E_K and E_L are the binding energies of the electrons in the K and L shells, respectively. The fluorescence yield, W, is a quantity that indicates the ratio of the number of X-rays emitted to the total number of vacancies in the K-shell; $W = X/(X + A)$, where X is the number of vacancies resulting in an X-ray, and A is the number of vacancies resulting in Auger electrons. The fluorescence yield is dependent on the atomic number of the nuclide.(22)

The decay scheme of cesium, Cs^{133}, following the decay of barium, Ba^{133}, by electron capture, has been studied extensively, and is shown in Figure 6.

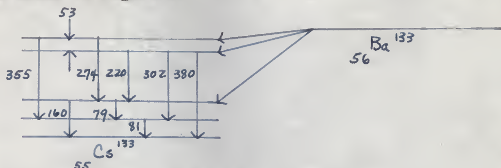

Figure 6

It was a convenient isotope to study with electron detectors because there was no continuous beta spectrum to obscure conversion electron peaks. On the other hand, due to the large number of transitions, there was some overlapping of lines. This can be seen in Table 2, where the transitions are listed with the corresponding K and L internal conversion electron energies of each transition. The 43, 45, and 48 Kev peaks could not be resolved; the 266 and 269, the 344 and 350, and

Transition Energy	K Line	L Line
53 Kev	17 Kev	48 Kev
79	43	74
81	45	76
160	124	155
220	184	215
274	238	269
302	266	297
355	319	350
380	344	375

Table 2

74 and 76 Kev lines appeared as single peaks. The complete conversion electron spectrum taken with the RCA detector at 77° K is shown on Plate I. Because the detectors were sensitive to photons, it was necessary to subtract the contribution

of X-rays and gamma rays from the total spectrum to give a true electron spectrum. This background spectrum was obtained by putting an absorber between the source and the detector which would stop all electrons but would not attenuate the photons appreciably. Plate II shows the background spectrum of Cs^{133}, which was subtracted from the total spectrum to give the electron spectrum shown in Plate I. It can be seen that low energy photons, the 31 Kev X-rays and the 80 Kev gamma rays, produce photopeaks, while higher energy photons contribute only by Compton scattering. The Compton edges of the intense 302 Kev and 355 Kev gamma rays show clearly.

One reason for studying this isotope was to determine whether the 53 Kev transition shown on the decay scheme actually existed. Since the L conversion line of this transition could not be resolved, it was necessary to search for the K conversion line at 17 Kev. Plate III shows the low energy portion of the electron spectrum. The peak at 23 Kev is believed to be Auger electrons, though their energy should be 25-26 Kev. Although a thin source was used, there may have been some self-absorption of these very low energy electrons which would decrease their observed energy. The intensity of this peak is surprising, considering the fact that the fluorescence yield for Z = 55 is 87%. The peak is seen to be symmetrical and has a resolution of 8 Kev. This would indicate that the peak is due to mono-energetic electrons and is not a composite of Auger electrons and K conversion electrons of the 53 Kev transition. The energy in channel 0 is 13 Kev, so the K line would be visible if it were present.

DESCRIPTION OF PLATE I

Ba^{133}; RCA detector, cooled; 40 minutes; 70 v, 4, 4, 1.5 v. The last four numbers in this description, and in the ensuing descriptions, refer, in order, to the detector bias, the main amplifier setting, the post amplifier setting, and the post bias. A background spectrum has been subtracted; the absorber thickness was 82.6 mg/cm^2.

PLATE I

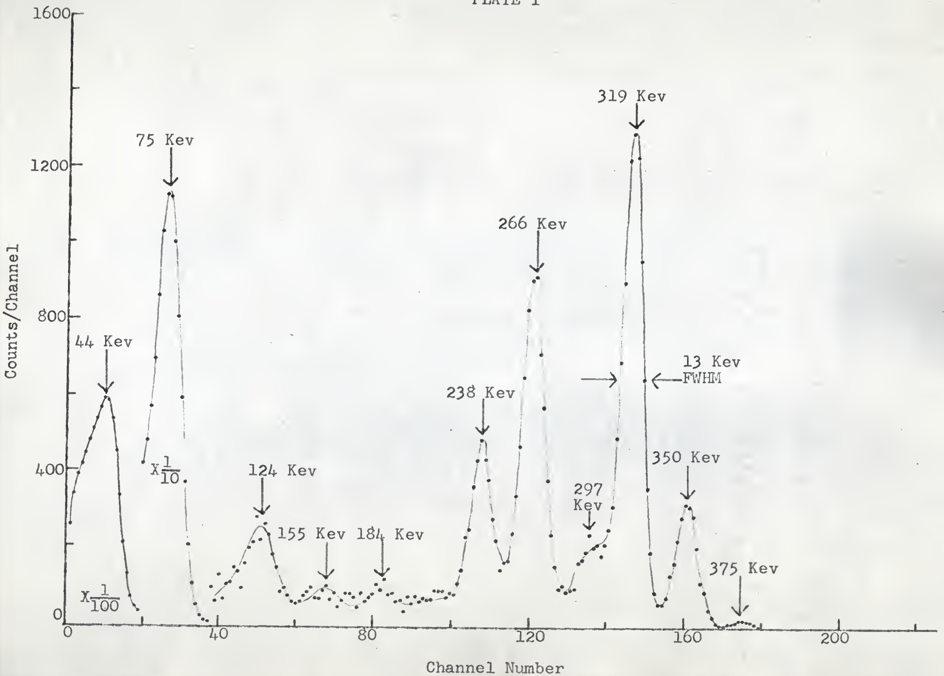

DESCRIPTION OF PLATE II

Background spectrum for Plate I; same conditions as for Plate I; 82.6 mg/cm^2 absorber

PLATE II

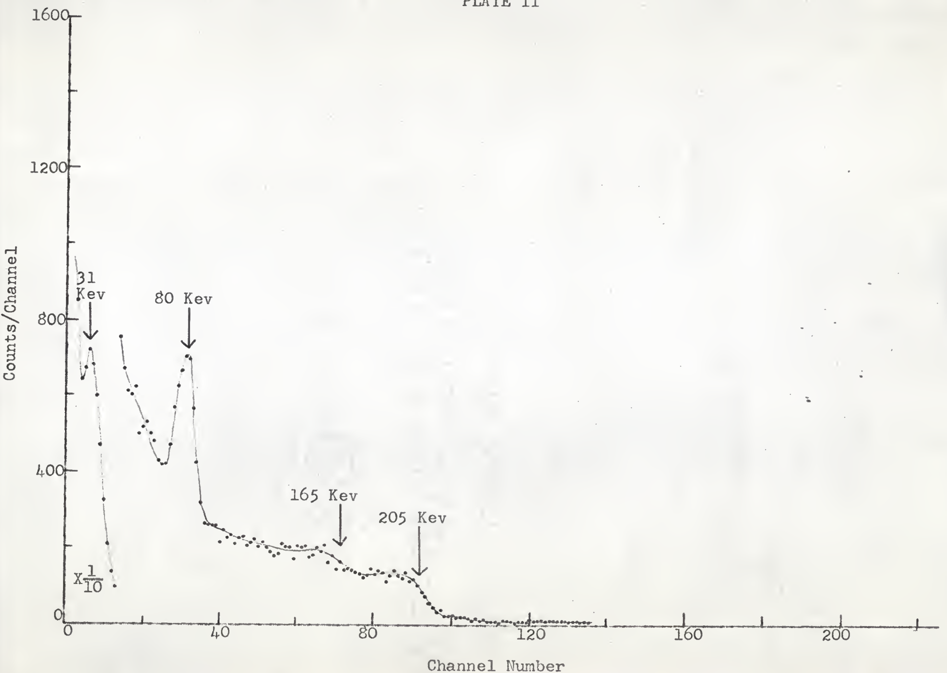

DESCRIPTION OF PLATE III

Ba^{133}; RCA detector, cooled; 10 minutes; 70 v, 4, 8, 1.0 v; background subtracted; 82.6 mg/cm^2 absorber

PLATE III

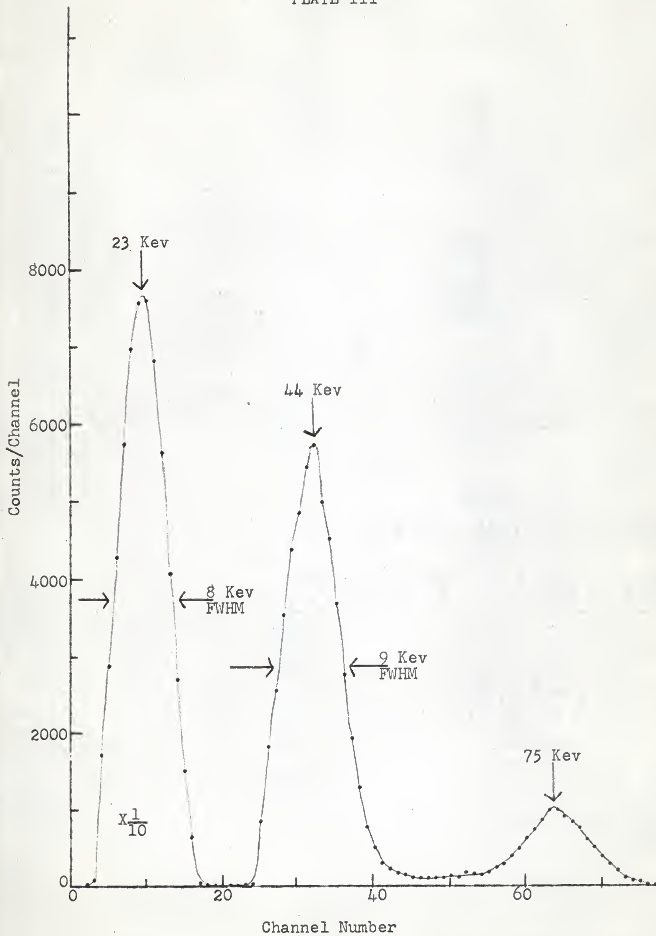

Plate IV is entered to show the high energy portion of the spectrum in more detail and to illustrate the good resolution of the Solid State Radiations detector at room temperature. The 297 Kev peak is not well resolved, but by folding over the high energy side of the 319 Kev peak about its center line, and subtracting the derived curve from the spectrum, the dashed peak at 297 Kev is obtained.

The decay scheme of indium, In^{115}, following the beta decay of cadmium, Cd^{115m}, was also investigated using semiconductor electron detectors. Most of the transitions are high in energy ($>$400 Kev), but transitions of 130, 162, and 291 Kev have been reported. However, no conversion electron peaks corresponding to these transitions were detected. Plate V shows the continuous beta spectrum of the decay of Cd^{115m}. The two peaks that do show on this plate, at 62 and 84 Kev, are the K and L conversion electron lines, respectively, of the 88 Kev transition of silver, Ag^{109}, which was present because the source contained some Cd^{109}. Cd^{109} decays by electron capture to Ag^{109}. The two peaks were not resolved completely when the detector was operated at room temperature. Plate VI shows the same spectrum with better resolution with the detector at 77° K. In the inset, which is obtained by subtracting the beta spectrum from the total spectrum, the peaks have a resolution of 10 Kev. The K/L ratio, determined by measuring the areas under the two peaks, was 0.76.

Cd^{115}, which has a half-life of 2.3 days, as compared to the 43 day activity of Cd^{115m}, has also been studied. It also decays to In^{115}, but to a completely different set of energy

DESCRIPTION OF PLATE IV

Ba^{133}; Solid State Radiations detector; 18 hours;
50 v, 4, 8, 10.5 v

PLATE IV

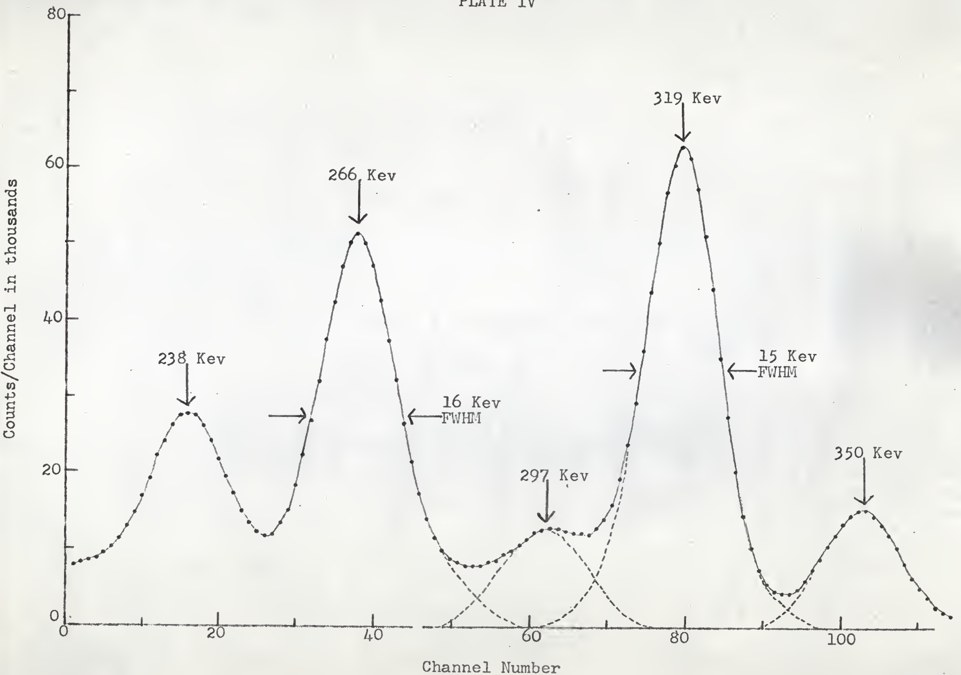

DESCRIPTION OF PLATE V

Cd^{109} and Cd^{115m}; RCA detector; 100 minutes; 40 v, 4, 8, 1.4 v

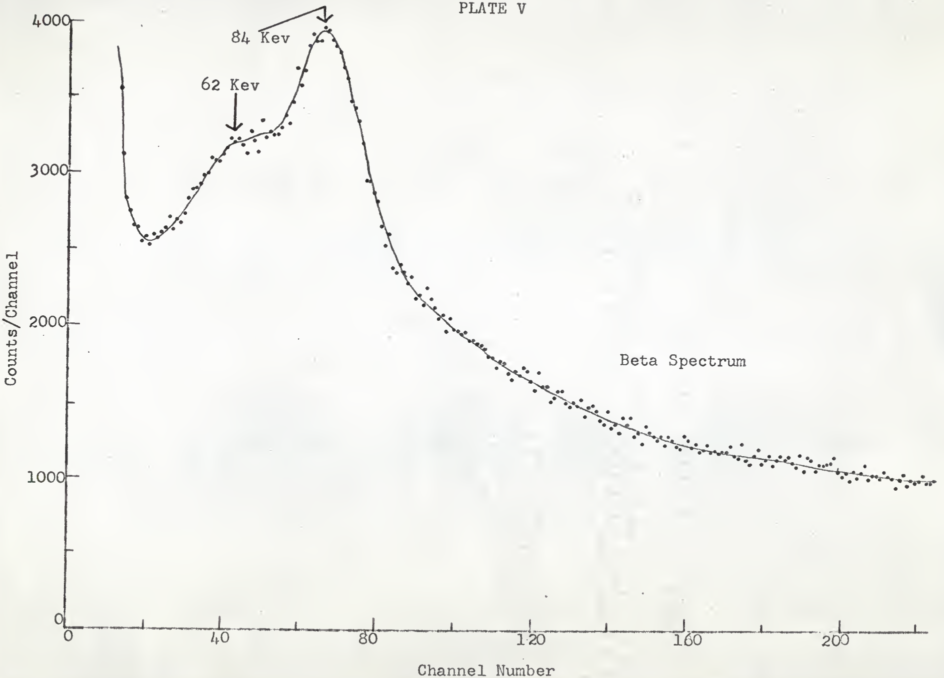

PLATE V
84 Kev
62 Kev
Beta Spectrum
Counts/Channel
4000
3000
2000
1000
0
0
40
80
120
160
200
Channel Number

DESCRIPTION OF PLATE VI

Cd^{109} and Cd^{115m}; RCA detector, cooled; 100 minutes; 40 v, 4, 8, 1.4 v; beta spectrum subtracted from upper curve to obtain lower curve

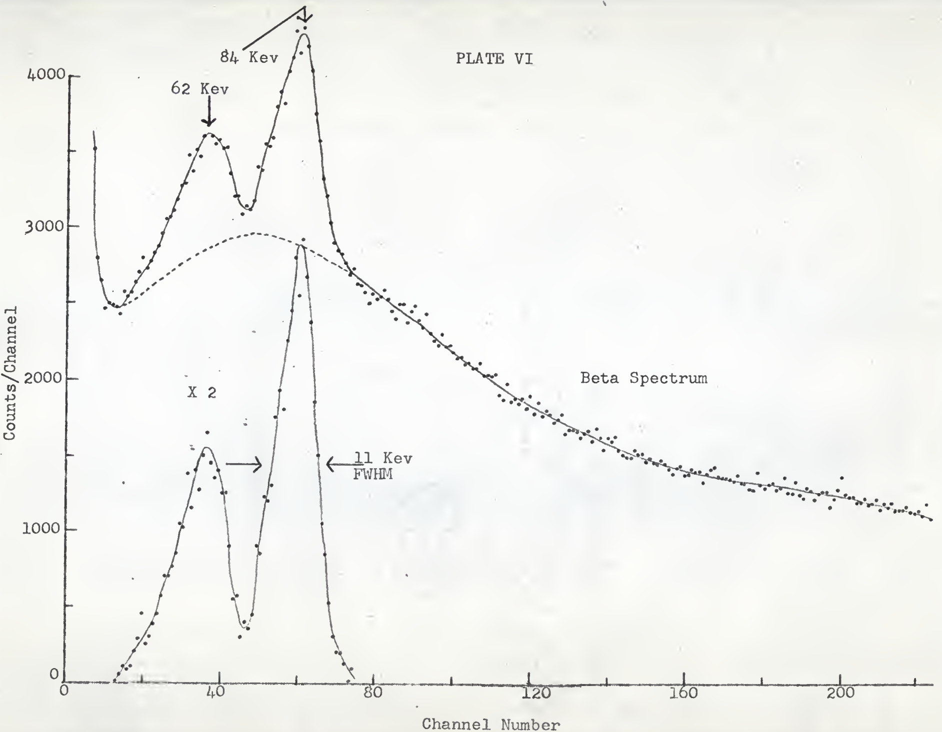
PLATE VI
84 Kev
62 Kev
Beta Spectrum
X 2
11 Kev
FWHM
Counts/Channel
Channel Number
0
1000
2000
3000
4000
40
80
120
160
200

levels. The conversion lines of a 335 Kev transition from a metastable state to the ground state, shown in Plates VII and VIII, were the only peaks observed. The lithium drifted p-i-n detector was used to scan the high energy region, but no conversion lines appeared on the beta spectrum.

One purpose of the study of Cd^{115} was to verify the existence of a 33 Kev transition, which would produce an L conversion line with an energy of 29 Kev in channel 17 on Plate IX. There is no indication that a peak is present in this area. The peak in channel 8 is due to Auger electrons, having an energy of 20 Kev. The conversion lines of the 335 Kev transition are just off the right edge of the plate.

Plates X, XI, and XII show the conversion lines of the 279 Kev transition of thallium, Tl^{203}, following the decay of mercury, Hg^{203}. Plate X was taken with the RCA detector at room temperature at 40 v bias, giving a K/(L + M) ratio of 3.0. Plate XII was taken with the same detector at 77° K at 40 v bias, yielding a K/(L + M) ratio of 2.5. One reason for the observed decrease of the ratio with temperature may be that the resistivity of silicon is increased by cooling due to its negative temperature coefficient, causing the width of the depletion layer to become greater and increasing the efficiency for the detection of the higher energy L and M conversion electrons, A wide variation in the K/(L + M) ratio has been reported: 2.57-3.2.(4)

Platinum, Pt^{197}, was produced in the Mark III Triga Reactor at Kansas State University by using Pt^{196} as the target material. This isotope has a half-life of 18 hours, decaying to gold, Au^{197}.

DESCRIPTION OF PLATE VII

Cd^{115}; RCA detector, cooled; 40 minutes; 70 v, 4, 8, 5.0 v; background subtracted, 547 mg/cm^2 absorber; background also shown

PLATE VII

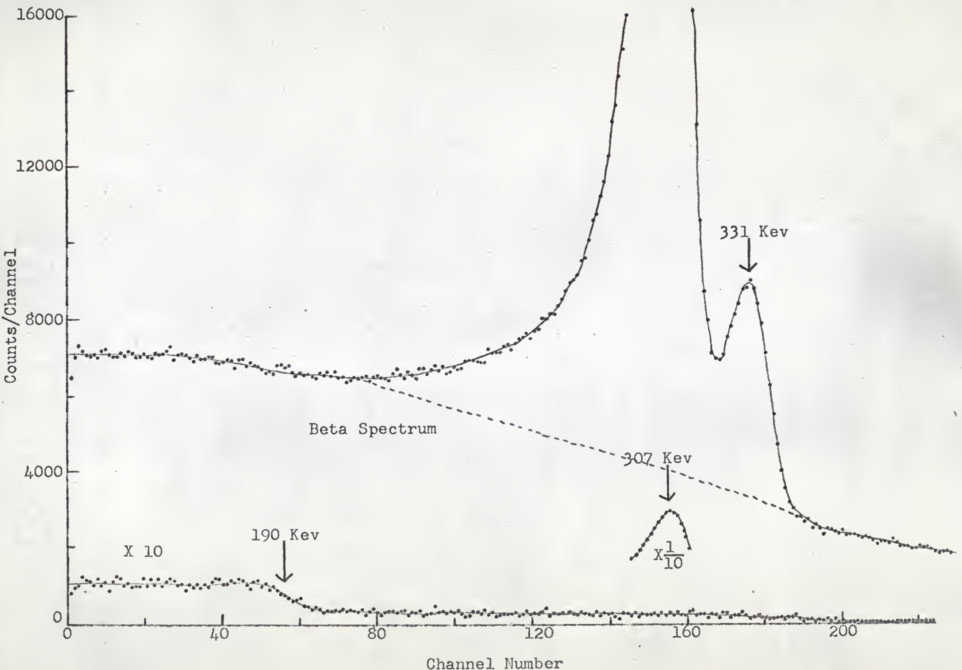

DESCRIPTION OF PLATE VIII

Cd^{115}; beta spectrum subtracted from Plate VII to show only conversion lines

PLATE VIII

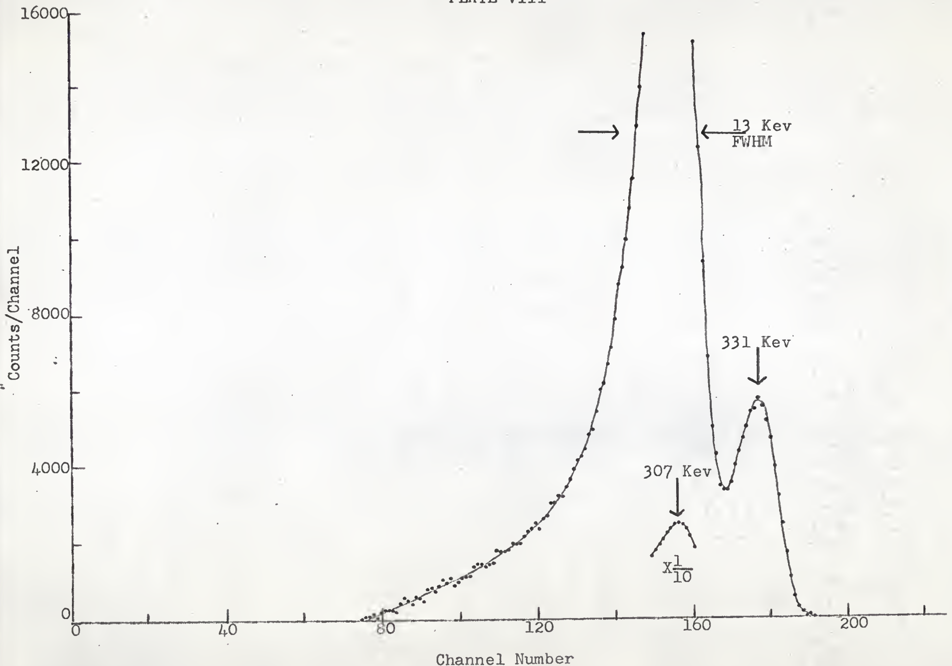

DESCRIPTION OF PLATE IX

Cd^{115}; RCA detector, cooled; 40 minutes; 70 v, 4, 8, 1.0 v; background subtracted, 547 mg/cm^2 absorber

PLATE IX

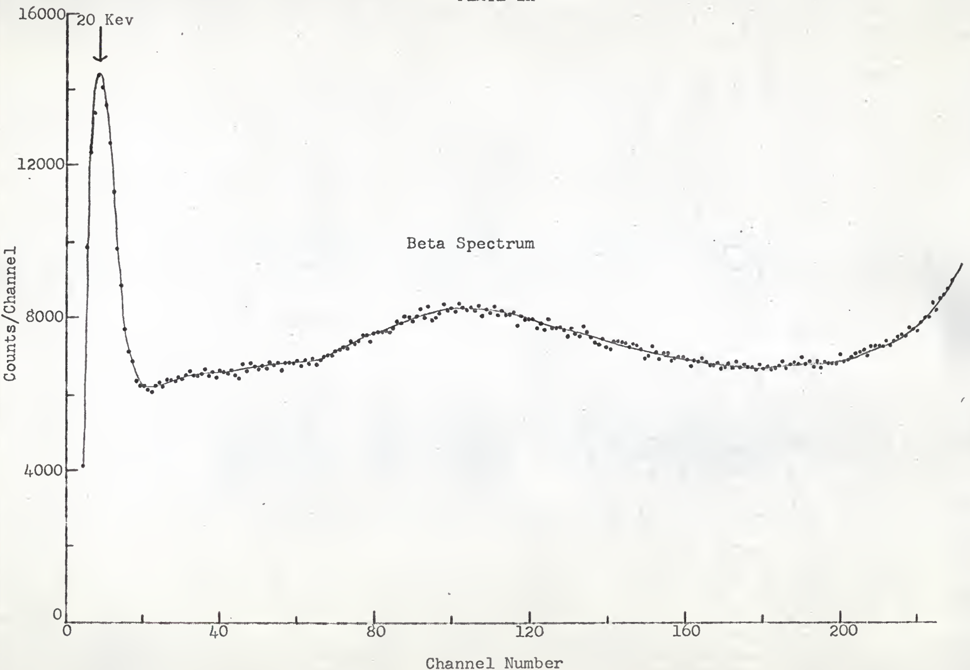

DESCRIPTION OF PLATE X

Hg^{203}; RCA detector; 100 minutes; 40 v, 4, 8, 5.0 v

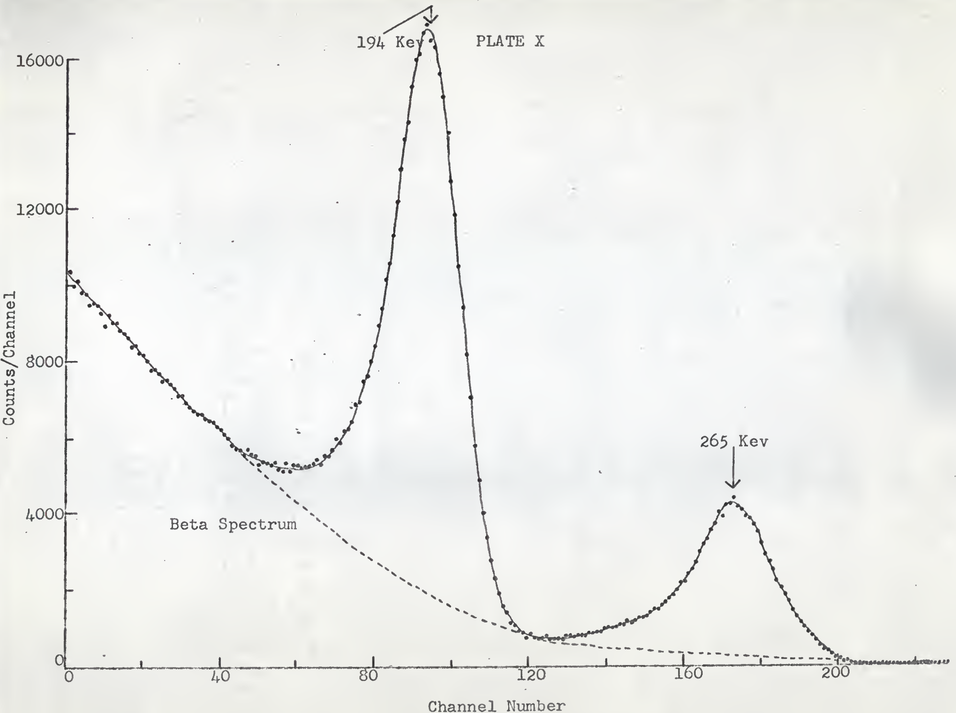
194 Kev
PLATE X
16000
12000
8000
4000
0
Counts/Channel
265 Kev
Beta Spectrum
0
40
80
120
160
200
Channel Number

PLATE XI

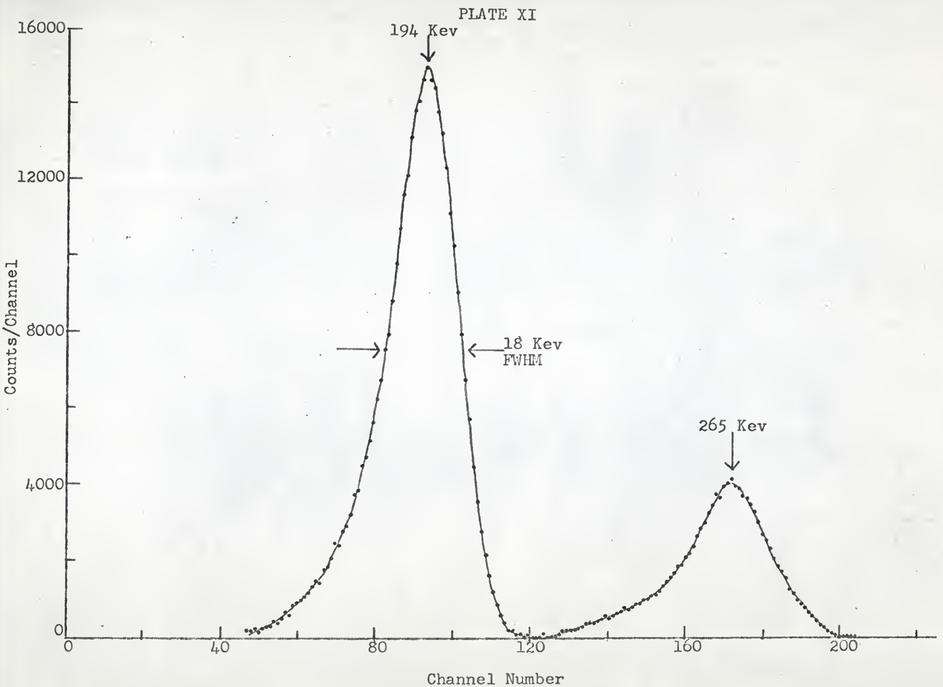

DESCRIPTION OF PLATE XII

Hg^{203}; RCA detector, cooled; 100 minutes; 40 v, 4, 8, 5.0 v; beta spectrum subtracted to show only conversion lines; K/(L + M) ratio, 2.5

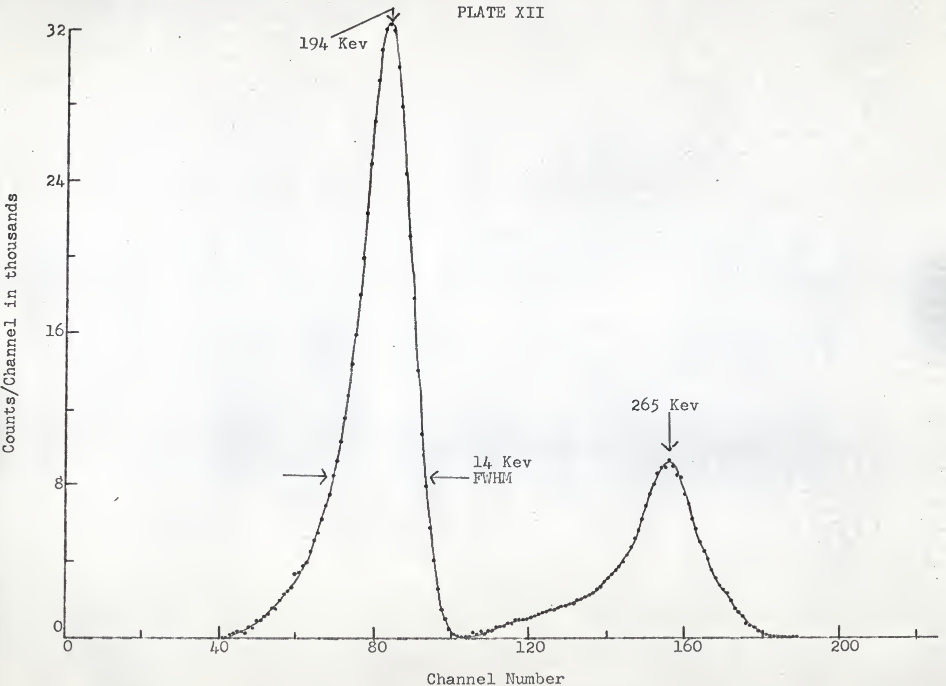
PLATE XII
194 Kev
14 Kev
FWHM
265 Kev
Counts/Channel in thousands
0
8
16
24
32
0
40
80
120
160
200
Channel Number

Some Pt^{197m} was also produced in the irradiation. This metastable state decays to Pt^{197} with a half-life of 78 minutes. Plate XIII is the electron spectrum taken within an hour after the sample was removed from the reactor. The peaks at 265 and 334 Kev are the K and L lines of the 346 Kev transition of Pt^{197m} to Pt^{197}. The peak at 64 Kev is the L conversion line of a 77 Kev transition in Au^{197}, and the peak at 110 Kev is the K conversion line of a 191 Kev transition in Au^{197}. The 265 and 334 Kev peaks do not show on Plate XIV, as the spectrum was taken 10 hours after the sample was irradiated, allowing the 78 minute activity to become negligible. The L line of the 191 Kev transition was never observed. The K line of the 77 Kev transition is energetically impossible, since the K binding energy of Au is greater than 77 Kev.

Plate XV is the conversion electron spectrum of lead, Pb^{207}, which is excited by the decay of $Bi^{207}$by electron capture. The K and L lines of the 570 and 1060 Kev transitions are shown. The spectrum was taken with the p-i-n detector, which yielded a resolution of only 30 Kev.

Bi^{207} is a useful isotope to measure, as the ratio of the 972 and 482 Kev peaks is well known, and this fact can be used to indicate whether a detector is thick enough to stop 1 Mev electrons.(11)

Plate XVI shows the conversion lines of the 661 Kev transition of Ba^{137} and the beta spectrum of the decay of Cs^{137} to Ba^{137} obtained with the Argonne detector. The K and L lines are not clearly resolved, but by employing the same techniques as used on Plate IV, the K and L lines may be separated as shown on Plate XVII .

DESCRIPTION OF PLATE XIII

Pt^{197} and Pt^{197m}; RCA detector; 10 minutes; 70 v, 4, 4, 2.1 v; beta spectrum subtracted from upper curve to obtain lower curve

PLATE XIII

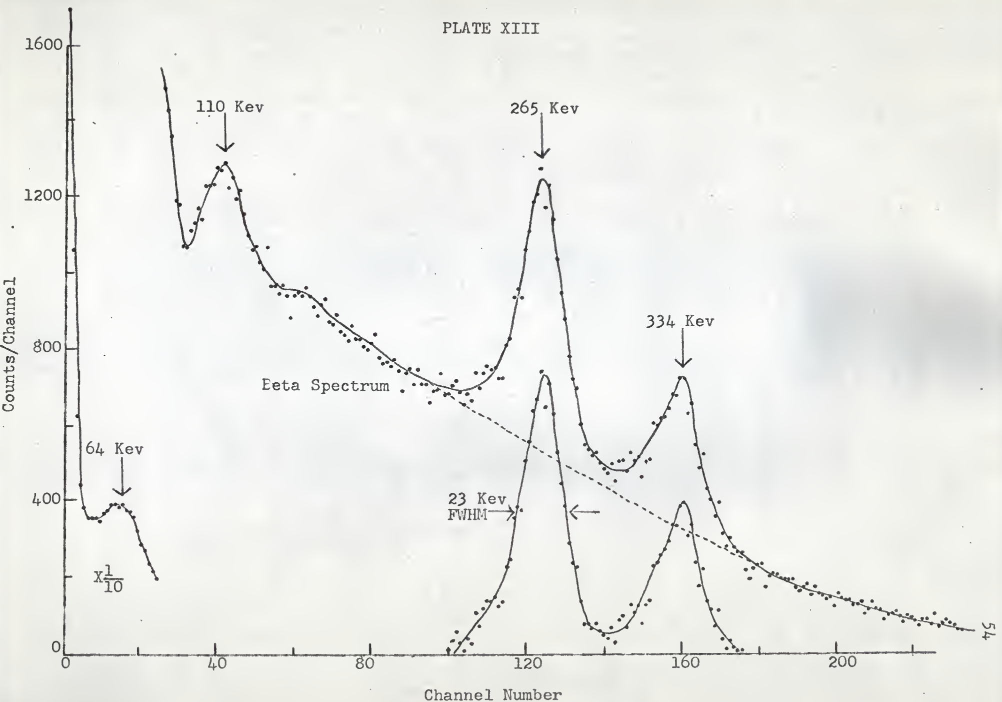

DESCRIPTION OF PLATE XIV

Pt^{197}; Solid State Radiations detector; 10 minutes; 50 v, 4, 8, 1.4 v; beta spectrum subtracted from upper curve to obtain lower curve

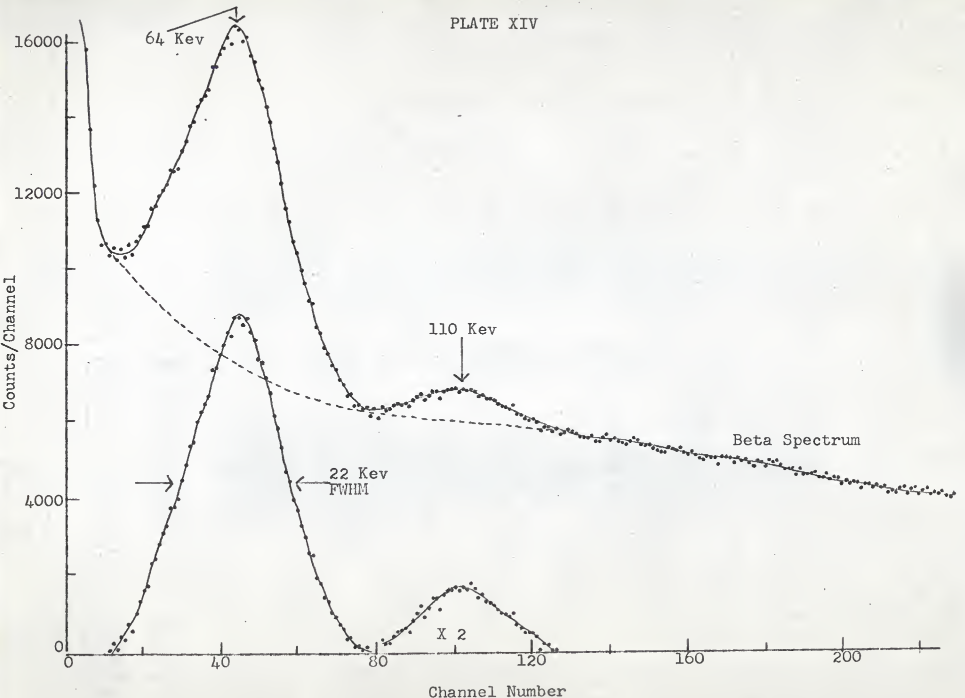
PLATE XIV
64 Kev
110 Kev
Beta Spectrum
22 Kev
FWHM
X 2
Counts/Channel
16000
12000
8000
4000
0
0
40
80
120
160
200
Channel Number

DESCRIPTION OF PLATE XV

Bi^{207}; Argonne p-i-n detector; 100 minutes; 100 v, 2, 4, 7.0 v; background subtracted; 438 mg/cm^2 absorber. The ratio of the intensities of the 972 and 482 Kev peaks is $\simeq$ 6.

PLATE XV

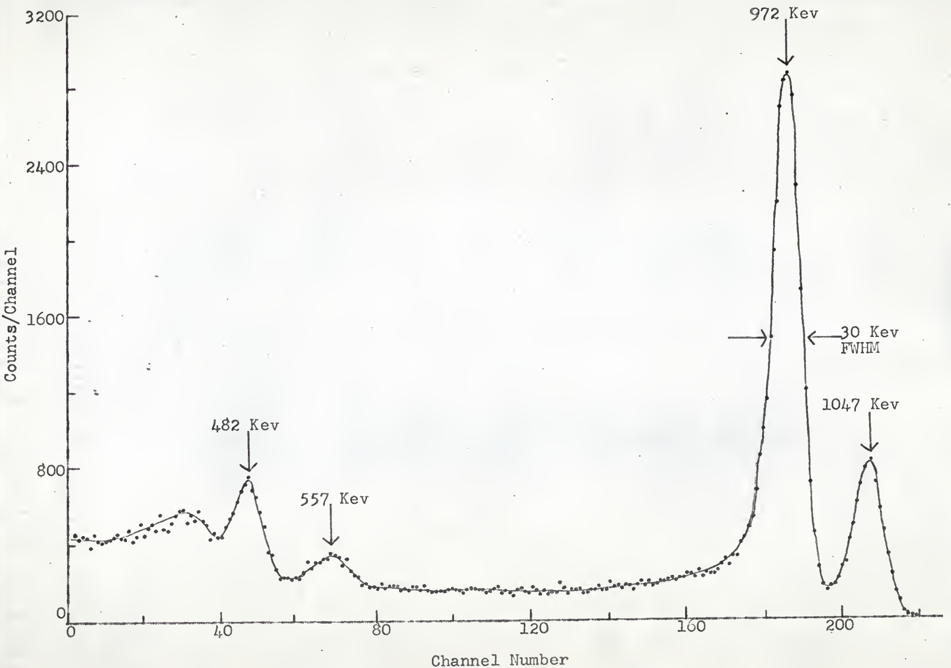

DESCRIPTION OF PLATE XVI

Cs^{137}; Argonne p-i-n detector; 80 minutes; 100 v, 2, 4, 2.0 v

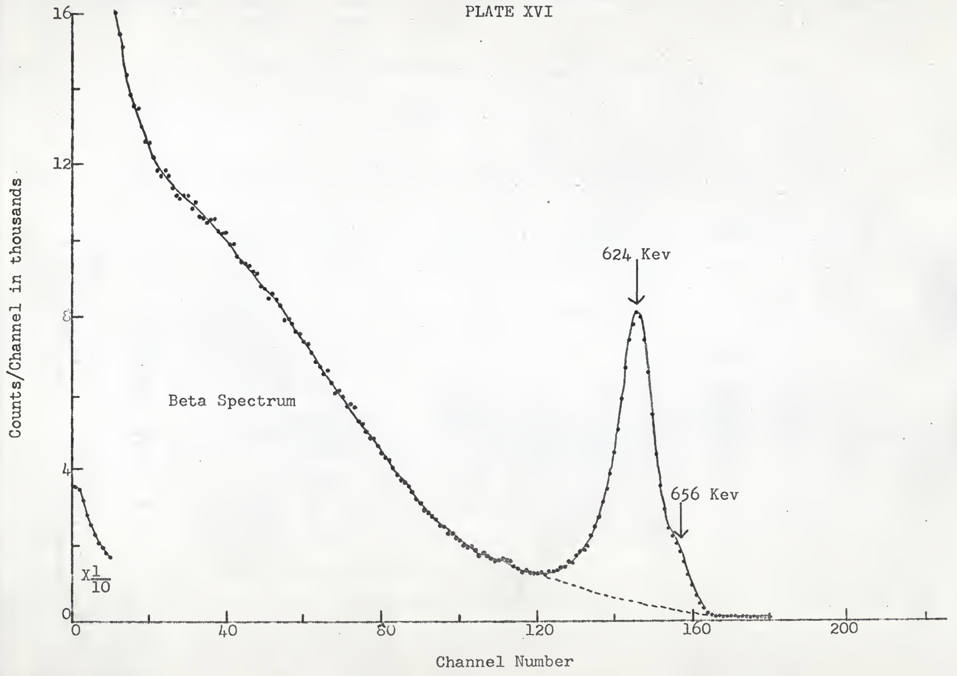
PLATE XVI
624 Kev
656 Kev
Beta Spectrum
X 1/10
Counts/Channel in thousands
0
4
8
12
16
Channel Number
0
40
80
120
160
200

DESCRIPTION OF PLATE XVII

Cs^{137}; beta spectrum subtracted from Plate XVI to show only conversion lines

PLATE XVII

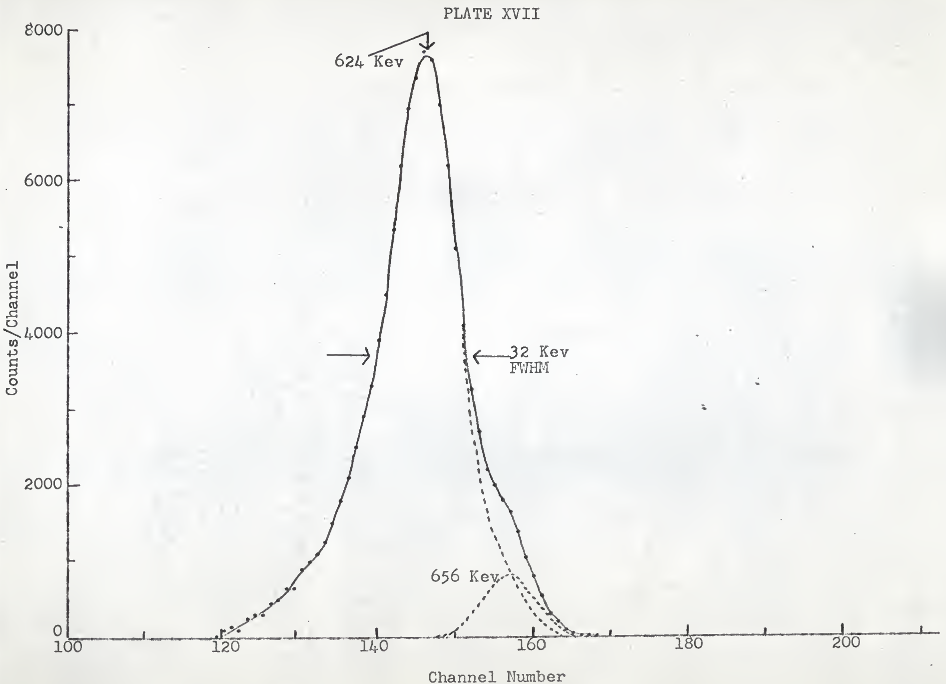

CONCLUSION

The semiconductor detectors used in this work have performed very well and have been instrumental in studying the decay schemes of several isotopes. When cooled to 77° K, the resolution obtained was limited by the electronic system, not the detectors. 15 Kev was the minimum electron energy that gave an output pulse larger than the noise level of the amplifier system. The detectors suffered no observable deterioration in the several months they were used. They were stored with no bias applied when not in use.

In addition to obtaining conversion electron and beta spectra, the solid state detectors were used in conversion electron-gamma ray coincidence experiments. The electron detector and source were mounted in the vacuum chamber as usual; a NaI(Tl) scintillation detector was then positioned next to the surface of the vacuum chamber.

Another application which would take advantage of the good resolution that can be obtained with semiconductor detectors and prove most useful in the study of nuclear decay schemes would be to do conversion electron - conversion electron coincidence experiments using 2 solid state detectors.

ACKNOWLEDGEMENTS

The author wishes to express his sincere thanks to Dr. Louis D. Ellsworth for his constant guidance and advice throughout this work, and to Dr. A. B. Cardwell for making the project possible.

LITERATURE CITED

1. Blankenship and Borkowski. Silicon Surface-Barrier Nuclear Particle Spectrometer. IRE Trans. on N. S., Vol. 7 No. 2-3 (June-Sept., 1960), p. 190

2. Blankenship and Borkowski. Improved Techniques for Making P+-I-N+ Diode Detectors. IRE Trans. on N. S., Vol. 9 No. 3 (June, 1962), p. 181

3. Bromley, D. A. Nuclear Experimentation with Semiconductor Detectors. IRE Trans. on N. S., Vol. 9 No. 3 (June, 1962), p. 135

4. Dzelepow and Peker. Decay Schemes of Radioactive Nuclei. Moscow: Academy of Sciences of the U. S. S. R. Press, 1958. pp. 606-07

5. Dunlap, W. C. An Introduction to Semiconductors. New York: John Wiley & Sons, Inc., 1957. pp. 150-51

6. Fox and Borkowski. Silicon Surface Barrier Detectors with High Reverse Breakdown Voltages. IRE Trans. on N. S., Vol. 9 No. 3 (June, 1962), p. 213

7. Friedland, Mayer, and Wiggins. The Solid State Ionization Chamber. IRE Trans. on N. S., Vol. 7 No. 2-3 (June-Sept., 1960), p. 181

8. Friedland, Mayer, and Wiggins. Tiny Semiconductor is Fast Linear Detector. Nucleonics, Vol. 18 No. 2 (Feb., 1960), p. 54

9. Kingston, R. H. Semiconductor Surface Physics. Philadelphia: Univ. of Penn. Press, 1957. pp. 139-43

10. Mann and Janarek. B^{10} Diffused Junction Detectors in N-type Silicon. IRE Trans. on N. S., Vol. 9 No. 3 (June, 1962), p. 200

11. Mann, Haslett, and Janarek. Lithium-drifted p-i-n Junction Detector. IRE Trans. on N. S., Vol. 9 No. 4 (Aug., 1962), p. 43

12. Mayer, J. W. The Development of the Junction Detector. IRE Trans. on N. S., Vol. 7 No. 2-3 (June-Sept., 1960), p. 178

13. Mayer, J. W. The State-of-the-Art in Nuclear Particle Detectors. IRE Trans. on N. S., Vol. 9 No. 3 (June, 1962), p. 124

14. McKenzie and Waugh. Silicon Junctions as Particle Spectrometers. IRE Trans. on N. S., Vol. 7 No. 2-3 (June-Sept., 1960), p. 185

15. Miller, Brown, Donovan and Mackintosh. Silicon p-n Junction Radiation Detectors. IRE Trans. on N. S., Vol. 7 No. 2-3 (June-Sept., 1960), p. 185

16. Pell, E. M. Ion Drift in an n-p Junction. Journal of Applied Physics, Vol. 31 (1959), p. 291

17. Shive, J. N. The Properties, Physics, and Design of Semiconductor Devices. Princeton: D. Van Nostrand Company Inc., 1959. pp. 287-94

18. Ibid., pp. 341-53

19. Siegbahn, Kai. Beta- and Gamm-Ray Spectroscopy. New York: Interscience Publishers Inc., 1955. pp. 628-30

20. Smith, R. A. Wave Mechanics of Crystalline Solids. New York: John Wiley & Sons Inc., 1961. p. 179

21. Walter, Dabbs, and Roberts. Semiconductor Particle Counters at Low Temperatures. IRE Trans. on N. S., Vol. 8 No. 1 (Jan., 1961), p. 79

22. Webb, Williams, and Jackson. An Encapsulated Silicon Junction Alpha-Particle Detector. IRE Trans. on N. S., Vol. 7 No. 2-3 (June-Sept., 1960), p. 199

23. White, G. K. Experimental Techniques in Low-Temperature Physics. Clarendon: Oxford, 1959. p. 41

24. Ziemba, Pelt, Ryan, Wang, and Alexander. Properties of an n^+-i-p^+ Semiconductor. IRE Trans. on N. S., Vol. 9 No. 3 (June, 1962), p. 155

THE USE OF SEMICONDUCTOR DEVICES IN NUCLEAR SPECTROSCOPY

by

DUANE K. FOWLER

B. A., University of South Dakota, 1961

AN ABSTRACT OF A MASTER'S THESIS

submitted in partial fulfillment of the

requirements for the degree

MASTER OF SCIENCE

Department of Physics

KANSAS STATE UNIVERSITY
Manhattan, Kansas

1963

ABSTRACT

Solid state devices have been used as electron detectors in the study of nuclear decay schemes. A lithium-drifted p-i-n detector, having a sensitive depth of nearly 2 mm, was employed for the detection of electrons having energies greater than 400 Kev. The detector did not give a linear response to electrons having less than 400 Kev because of a 25 micron window. The internal conversion spectra of Bi^{207} and Cs^{137} were taken. The resolution (full width at half maximum) obtained was 30 Kev, which was not sufficient to resolve the K and L conversion lines of Cs^{137}.

Two silicon p-n junction diodes, having windows of 1 micron and 0.1 micron, respectively, and depletion layers of about 400 microns, were used for the detection of electrons having energies less than 400 Kev. The resolution obtained with these detectors at room temperature was 15-17 Kev. Signals from electrons having less than 30 Kev of energy were obscured by the noise generated in the detector and the preamplifier. When cooled to 77° K, 8-10 Kev resolution was realized, and the minimum electron energy which gave a signal larger than the noise level was 15 Kev. It was found necessary to cool the detectors prior to the application of a reverse bias.

Internal conversion spectra of Ba^{133}, Cd^{109}, Cd^{115}, Cd^{115m}, Pt^{197}, and Hg^{203} have been studied. No evidence was found to verify the existence of a 53 Kev transition in Cs^{133} following the decay of Ba^{133}. Conversion lines from all the other transitions and Auger electrons have been obtained. The K/L ratio

of the 88 Kev transition in Ag^{109} following the decay of Cd^{109} was measured to be 0.76. No conversion peaks could be detected in the electron spectrum of In^{115} following the beta decay of Cd^{115m}. Following the decay of Cd^{115}, which excites an entirely different set of energy levels in In^{115}, conversion lines of the 335 Kev transition, the L line of the 33 Kev transition, and Auger electrons have been detected. Pt^{196} was irradiated to produce Pt^{197}, which decays to Au^{197} with a half-life of 18 hours. An isomeric state is also excited in Pt^{197} during the irradiation; this state decays to the ground level with a half-life of 78 minutes. The conversion lines of the 345 Kev transition in Pt^{197}, the L line of the 77 Kev transition and the K line of the 191 Kev transition in Au^{197} have been observed. The K/(L + M) ratio of the conversion lines of the 279 Kev transition in Tl^{203}, which follows the decay of Hg^{203}, has been measured to be 2.5.